

Correction of multi-gene deficiency *in vivo* using a single 'self-cleaving' 2A peptide-based retroviral vector

Andrea L Szymczak^{1,3,4}, Creg J Workman¹, Yao Wang¹, Kate M Vignali¹, Smaroula Dilioglou¹, Elio F Vanin^{2,5} & Dario A A Vignali^{1,4}

Attempts to generate reliable and versatile vectors for gene therapy and biomedical research that express multiple genes have met with limited success. Here we used Picornavirus 'self-cleaving' 2A peptides, or 2A-like sequences from other viruses^{1–3}, to generate multicistronic retroviral vectors with efficient translation of four cistrons. Using the T-cell receptor:CD3 complex as a test system, we show that a single 2A peptide-linked retroviral vector can be used to generate all four CD3 proteins (CD3 ϵ , γ , δ , ζ), and restore T-cell development and function in CD3-deficient mice. We also show complete 2A peptide-mediated 'cleavage' and stoichiometric production of two fluorescent proteins using a fluorescence resonance energy transfer-based system in multiple cell types including blood, thymus, spleen, bone marrow and early stem cell progenitors.

Conventional approaches for the production of multicistronic vectors using internal ribosomal entry sites (IRES) or other promoters are problematic because multiple proteins are often not expressed at the same level. Several viruses use 2A peptides, or 2A-like sequences, to mediate protein cleavage^{2,4}. These include members of the Picornaviridae virus family, such as foot-and-mouth disease virus (FMDV) and equine rhinitis A virus (ERAV), and other viruses such as the porcine teschovirus-1 and the insect virus *Thosea asigna* virus (TaV)³. The 2A peptide consensus motif (2A, Asp-Val/Ile-Glu-X-Asn-Pro-Gly; 2B, Pro) is extremely rare and is always associated with cleavage activity between the 2A glycine and the 2B proline (Fig. 1a). Through a ribosomal skip mechanism, the 2A peptide impairs normal peptide bond formation between the 2A glycine and the 2B proline without affecting the translation of 2B⁵. We chose to assess the unique properties of the 2A peptide sequence using the T-cell receptor (TCR):CD3 complex as a test system. This is a large, multichain complex that is composed of at least eight different subunits (TCR α :TCR β , CD3 ϵ :CD3 γ , CD3 ϵ :CD3 δ and CD3 ζ :CD3 ζ), all of which are necessary for efficient TCR:CD3 complex surface expression and for T-cell development and function⁶.

The 2A peptide regions from FMDV (abbreviated herein as F2A),

ERAV (E2A) and TaV (T2A) were used to generate several multicistronic cassettes which linked the CD3 $\epsilon\gamma\delta\zeta$ or TCR $\alpha\beta$ chains to make a single fragment encoding two, three or all four proteins (Fig. 1a,b and Supplementary Fig. 1 online). The cassettes were subcloned into pCIneo (for *in vitro* transcription/translation experiments) or a murine stem cell virus (MSCV)-based retroviral vector, which contains an IRES and green, yellow or cyan fluorescent protein (GFP, YFP or CFP; referred to herein as pMIG, pMIY or pMIC, respectively, for the vectors and as MIG, MIY and MIC when referring to the resulting virus)⁷ (Fig. 1b). Because retroviruses are known to recombine vector sequences that contain duplications of homologous regions^{8,9}, different 2A peptide sequences with silent mutations were used within the constructs containing three or four 2A peptide-linked cistrons (Fig. 1a and Supplementary Fig. 1 online).

To verify that the proteins were made and cleaved efficiently, we coupled *in vitro* transcription and translation with the CD3 $\delta\gamma$ -2A constructs (Fig. 1c). Translated products were detected by western blot analysis using streptavidin and the band identities were confirmed by probing with anti-sera to CD3 δ and CD3 γ (Fig. 1c). Migration of the translation products was consistent with their predicted molecular weight and charge (Fig. 1c, lanes 2 and 3). A noncleaving version of CD3 $\delta\gamma$ -T2A was made by mutating the last proline and glycine of the T2A peptide region to alanine³ (underlined in Fig. 1a), and was used to indicate the position of any uncleaved material (Fig. 1c, lane 4). Each of the CD3 $\delta\gamma$ -2A linked vectors produced a single, intense band corresponding to CD3 δ -2A and CD3 γ , which comigrate owing to the addition of the 2A peptide sequence on CD3 δ (Fig. 1c, lanes 5–7). Notably, with the exception of a faint band seen with the E2A-linked construct, no uncleaved CD3 $\delta\gamma$ -2A could be found, indicating close to 100% cleavage. These results show that the 2A peptides mediate highly efficient generation of individual CD3 chains in this *in vitro* translation system.

Cell surface expression of TCR:CD3 complexes was analyzed by transient transfection of 293T cells with different combinations of single and 2A peptide-linked constructs¹⁰. Efficient cell surface expression of the TCR complex requires the presence and correct assembly of all six TCR:CD3 chains⁶, as shown by flow cytometric analysis

¹Department of Immunology and ²Division of Experimental Hematology, Department of Hematology/Oncology, St. Jude Children's Research Hospital, 332 N. Lauderdale, Memphis, Tennessee 38105, USA. ³Graduate Program in Pathology and ⁴Department of Pathology, University of Tennessee Medical Center, 62 S. Dunlap, Memphis, Tennessee 38163, USA. ⁵Present address: Center for Cell and Gene Therapy, Baylor College of Medicine, 6621 Fannin Street, Houston, Texas 77030, USA. Correspondence should be addressed to D.A.A.V. (dario.vignali@stjude.org).

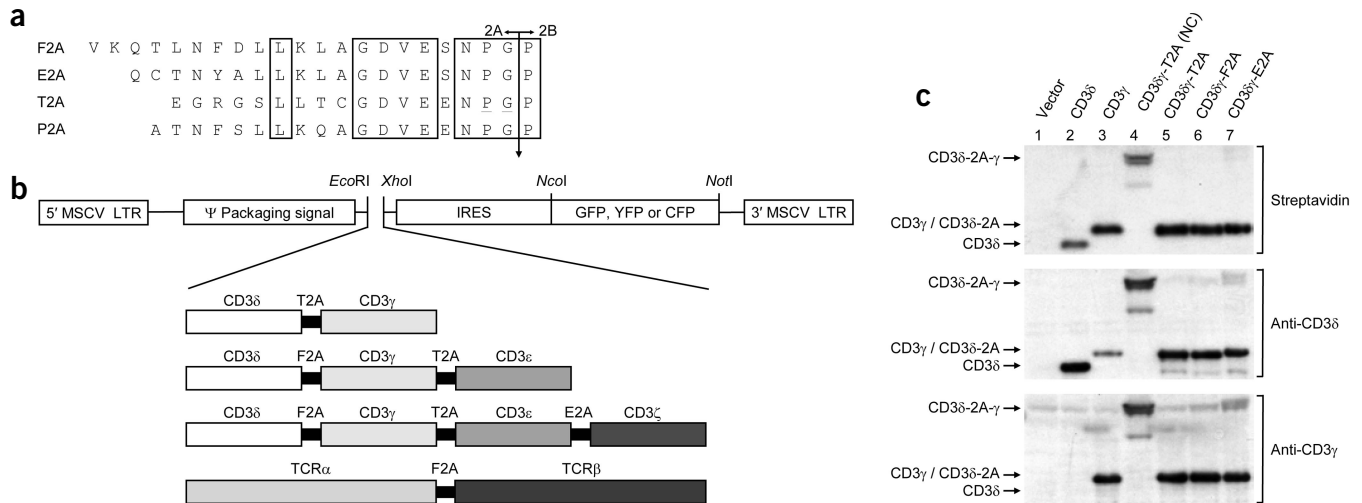


Figure 1 Construction and processing of 2A-linked TCR:CD3 constructs. **(a)** Amino acid sequence of the 2A regions of foot-and-mouth disease virus (F2A), equine rhinitis A virus (E2A), *Thoesa asigna* virus (T2A) and porcine teschovirus-1 (P2A; used later in FRET analysis). Conserved residues are boxed. Underlined amino acids were mutated to alanine for generation of a noncleaving construct. The cleavage point between the 2A and 2B peptides, and thus the N- and C-terminal cistrons, is indicated by the arrow. **(b)** Schematic of the retroviral vector and 2A-linked TCR:CD3 constructs used. The MSCV long terminal repeat promoter is used to express the 2A-linked construct. The IRES is used to direct translation of GFP. Key restriction sites used for cloning are noted. **(c)** *In vitro* transcription/translation of single or 2A-linked CD3 chains. Proteins were translated in the presence of biotinylated lysine and detected by western blot analysis with streptavidin (top). Identity of translation products was confirmed by western blot analysis with rabbit anti-CD3 δ (middle) or anti-CD3 γ (bottom) antisera. Note that the anti-CD3 δ antisera weakly cross-reacts with CD3 γ . Migration of translation products was consistent with their predicted molecular weight and charge (CD3 δ , $M_r = 19,032/pI = 6.41$; CD3 γ , $M_r = 20,252/pI = 9.03$; CD3 δ -2A, $M_r = 20,747/pI = 5.57$; CD3 δ -2A- γ , $M_r = 41,078/pI = 7.50$). Note that the 2A tag, which remains attached to CD3 δ (the N-terminal protein), affects protein migration and thus results in the comigration of CD3 γ and CD3 δ -2A. As these proteins were translated in the absence of endoplasmic reticulum, they have not been processed and migrate differently from the native proteins (see Fig. 2c). Differences in band intensity between CD3 δ and CD3 γ are likely due to lysine content (9 and 13, respectively). NC, noncleaving.

(Supplementary Fig. 2 online). The percentage of TCR⁺CD3⁺ cells observed with the 2A peptide-linked constructs was greater than or equal to that obtained with the separate TCR:CD3 constructs (Fig. 2a, top panel and Supplementary Fig. 2 online). Indeed, effective surface TCR expression could be achieved with just two plasmids. Efficient cleavage of the 2A peptide-linked constructs was clearly shown to be essential for surface TCR:CD3 expression by analysis of the noncleaving CD3 $\delta\gamma$ -2A(NC) construct (Fig. 2a, bottom panel).

To determine if the 2A peptide-linked constructs can be stably expressed, we made high titer retroviral producers for each of the individual TCR:CD3 vectors and four of the 2A peptide-linked constructs. Stable, high level TCR:CD3 cell surface expression on 3T3 cells was obtained after transduction with just two retroviruses (TCR $\alpha\beta$ -2A + CD3 $\delta\gamma\zeta$ -2A) (Fig. 2b). The identity of the assembled proteins was confirmed by surface biotinylation and western blot analysis with chain-specific antibodies (Fig. 2c). All constructs, except for TCR β and CD3 ζ , have a 2A peptide attached to their C terminus, and thus migrate differently from the wild-type proteins. This represents a useful way to distinguish between the recombinant and endogenous proteins.

The 2A peptide-linked CD3 constructs were further tested for their ability to reconstitute TCR expression in CD3-deficient mice by retroviral-mediated stem cell gene transfer. CD3 $\epsilon^{\Delta P/\Delta P}$ mice lack CD3 ϵ and have a severe inhibition of CD3 γ and CD3 δ gene expression leading to a complete arrest in T-cell development at the CD44⁺CD25⁺ double negative (CD4⁺CD8⁻) stage¹¹. These mice were crossed with CD3 $\zeta^{-/-}$ mice to generate mice that lack all four CD3 chains (CD3 $\epsilon^{\Delta P/\Delta P}$ × CD3 $\zeta^{-/-}$ mice^{11,12}). We examined the ability of

the CD3 $\delta\gamma\zeta$ -2A construct to reconstitute T-cell development in these mice. Lethally irradiated CD3 $\epsilon^{\Delta P/\Delta P}$ × CD3 $\zeta^{-/-}$ mice were used as recipients throughout. Bone marrow from C57BL/6 and CD3 $\epsilon^{\Delta P/\Delta P}$ × CD3 $\zeta^{-/-}$ mice transduced with MIG retrovirus served as positive and negative controls, respectively. As expected, T-cell development was restored in C57BL/6 but not in CD3 $\epsilon^{\Delta P/\Delta P}$ × CD3 $\zeta^{-/-}$ recipients (Fig. 3a, left and center dot plots, respectively). In contrast, the percentage of T cells in recipients of CD3 $\delta\gamma\zeta$ -2A.MIG-transduced CD3 $\epsilon^{\Delta P/\Delta P}$ × CD3 $\zeta^{-/-}$ bone marrow was comparable to the C57BL/6 positive control. Essentially all the T cells in CD3 $\delta\gamma\zeta$ -2A.MIG-transduced CD3 $\epsilon^{\Delta P/\Delta P}$ × CD3 $\zeta^{-/-}$ mice were GFP⁺ and only expressed the 2A-tagged CD3 ϵ (Fig. 3a and 3b, respectively). This result demonstrates that efficient expression and cleavage of the CD3 $\delta\gamma\zeta$ -2A construct was required for effective T-cell development.

Although fewer GFP⁺ cells were recovered from the spleen of CD3 $\epsilon^{\Delta P/\Delta P}$ × CD3 $\zeta^{-/-}$ than from C57BL/6 bone marrow recipients, transduction efficiency was comparable (Fig. 3c, left hand bars and upper right corner, respectively). Notably, the number of GFP⁺ T cells relative to the total number GFP⁺ cells was the same, if not slightly higher in spleens from CD3 $\delta\gamma\zeta$ -2A reconstituted mice compared with MIG-C57BL/6 controls (Fig. 3c, black versus gray bars, respectively). TCR surface expression was high but slightly lower in the CD3 $\delta\gamma\zeta$ -2A reconstituted mice (Fig. 3d). Finally, T cells expressing the CD3 $\delta\gamma\zeta$ -2A construct proliferated effectively after stimulation with anti-TCR antibody (Fig. 3e). Similar experiments were also performed in CD3 $\epsilon^{\Delta P/\Delta P}$ mice using single or 2A peptide-linked vectors with comparable results (Supplementary Fig. 3 and Supplementary Table 1 online). These experiments clearly show that transduction

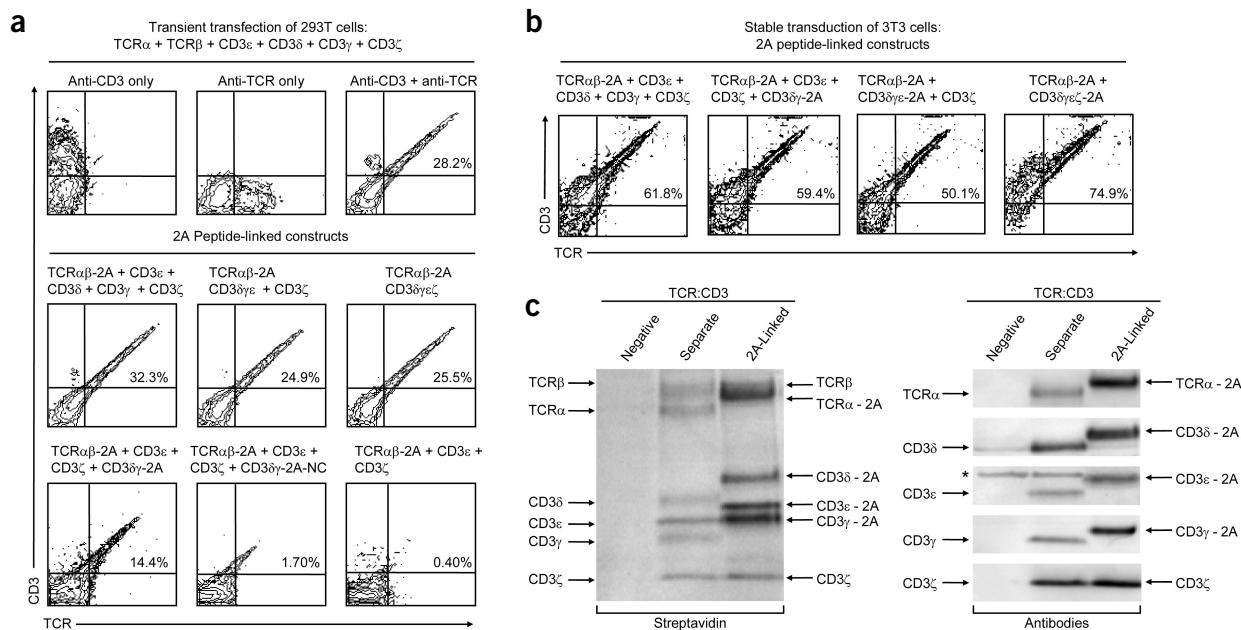


Figure 2 Efficient cleavage and expression of TCR:CD3 complexes on 293T and 3T3 cells using 2A-linked vectors. **(a)** 293T cells were transiently transfected with plasmids carrying the individual or 2A-linked TCR:CD3 chains indicated. Cells were stained with anti-TCR- β , PE, anti-CD3, APC or both and analyzed by flow cytometry. The percentage of live, TCR⁺CD3⁺ cells is shown. **(b)** Supernatant from retroviral producers expressing 2A peptide-linked TCR:CD3 chains was used to transduce 3T3 cells. Cells were analyzed as in **a**. **(c)** 3T3 cells transduced with separate or 2A-linked TCR:CD3 chains were surface biotinylated and lysed in digitonin. Untransduced cells were used as a control (negative). Lysates were immunoprecipitated with anti-TCR- β and the eluted proteins resolved by SDS-PAGE. Membranes were probed with streptavidin or antibodies. *, a nonspecific ~26–27 kDa band was observed in both the negative and transduced cells after western blot with anti-CD3 ϵ .

efficiency was extremely low and variable when using three different producers, emphasizing the benefits of using 2A peptide-linked multicistronic vectors.

To assess the efficiency of cleavage in multiple cell types and the stoichiometry between the cleaved products, we used fluorescence resonance energy transfer (FRET), which has been used extensively to assess the proximity of two proteins. FRET occurs when the energy state of an excited donor fluorophore (CFP) is transferred to an acceptor fluorophore (YFP) that is within 60–100 Å¹³. This allows for the direct assessment of the distance between CFP and YFP in unmanipulated cells. If a FRET signal is detected, then the two proteins are in close physical proximity, whereas the absence of FRET indicates a lack of association.

We tested three groups of mice that were generated by retroviral-mediated stem cell gene transfer. In the test group, mice expressed a 2A peptide-linked CFP/codon-diversified YFP (YFP^{CD}) cassette (CFP-2A-YFP^{CD}) (Fig. 4a). To prevent recombination between the nearly identical CFP and YFP proteins, a YFP^{CD} variant was made by introducing all possible silent mutations within each amino acid codon (Supplementary Fig. 4 online). We anticipated that there would be an inverse relationship between the degree of FRET observed in cells expressing the CFP-2A-YFP^{CD} construct and the efficiency of cleavage. We used a single vector that contained both CFP and YFP connected by a linker (CFP-link-YFP^{CD}), as a positive control, to allow for maximal observed FRET. Mice were generated using a 50:50 combination of retroviral producers expressing either CFP or YFP^{CD} in separate vectors, as a negative control. Because these two fluorescent proteins are not connected, FRET should not be observed.

Six to eight weeks post-transfer, we examined multiple cell types in the blood, thymus, spleen and bone marrow and determined the level

of FRET (Fig. 4b and Fig. 4c). As expected, random expression of CFP and YFP^{CD} was observed in thymocytes expressing the individual fluorescent proteins (Fig. 4b, upper left panel). In contrast, concordant expression of CFP and YFP^{CD} was observed with the CFP-link-YFP^{CD} and the CFP-2A-YFP^{CD} constructs (Fig. 4b, upper middle and right panels). Whereas strong FRET was observed with CFP-link-YFP^{CD} expressing cells, FRET was not detected in cells expressing the individual proteins (Fig. 4b, lower left and middle panels). Notably, the 2A peptide-linked CFP/YFP^{CD} cells did not show FRET and were comparable to the negative control in all tissues examined (Fig. 4b, lower right panel and Fig. 4c). These results were extended to various subpopulations of cells within these tissues for both lymphoid and non-lymphoid lineages as well as in c-kit⁺CD34⁻Lin⁻ stem cells in the bone marrow (Supplementary Fig. 5 online). Importantly, the amount of CFP and YFP^{CD} produced after 2A peptide cleavage was nearly equal, as indicated by western blot analysis of B cells from the CFP-2A-YFP^{CD} mice (Fig. 4d). This indicates the near stoichiometric production of 2A peptide-linked proteins.

Our data clearly demonstrate that 2A peptides can be used for the stoichiometric coexpression of at least four different proteins *in vitro* and *in vivo*. Expression of the 2A peptide-linked proteins appears to be very stable in cell lines and mice. In separate studies, long-term, stable expression of 2A peptide-linked TCR $\alpha\beta$ proteins in mice was seen up to 7 months post-transfer (P. Arnold, A. Burton and D.A.A.V., unpublished data). Finally, FRET analysis confirmed efficient cleavage and stoichiometric expression of 2A peptide-linked proteins in multiple cell types including early stem cell progenitors. Although we have used 2A peptides to generate multicistronic retroviral vectors, it seems likely that these could also be used in other gene therapy delivery systems such as recombinant adeno-associated virus (rAAV) and Venezuelan

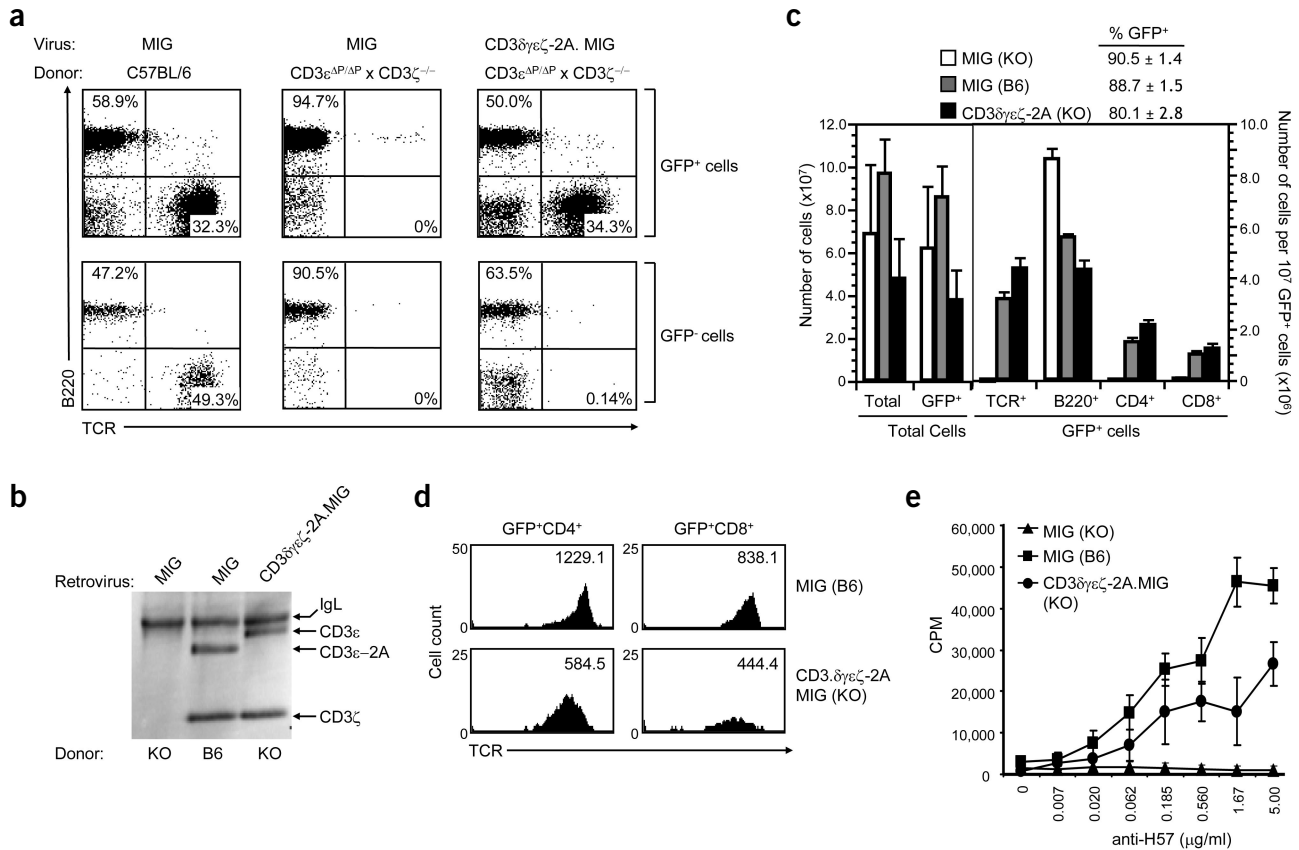


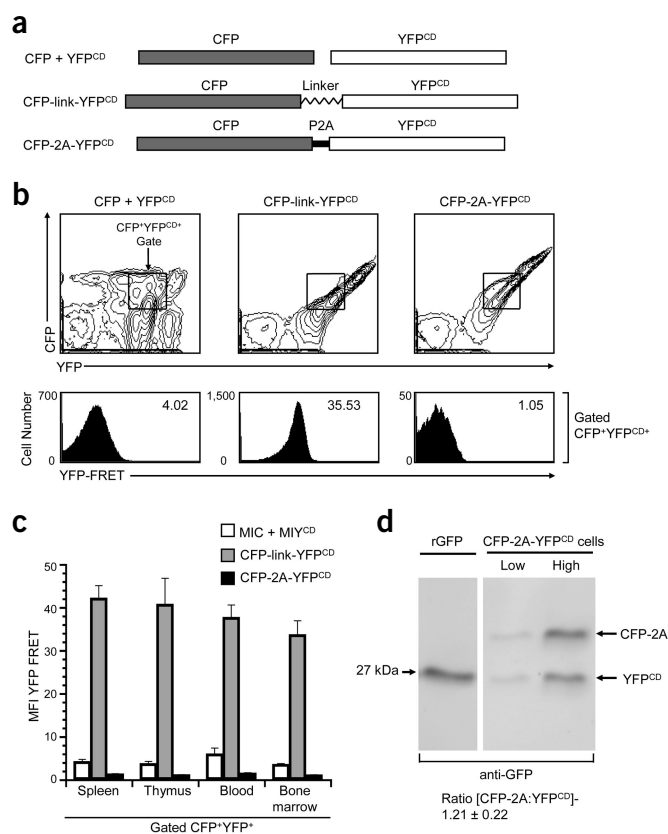
Figure 3 T-cell reconstitution in mice lacking all four CD3 molecules using a single, 2A-linked, multicistronic retroviral vector. **(a)** Splenocytes were stained with antibodies against TCR- β and B220, gating on live, GFP⁺ or GFP⁻ populations. A representative dot plot from each group is shown. **(b)** Splenocytes were lysed in digitonin and TCR:CD3 complexes immunoprecipitated with anti-TCR- β . Eluted proteins were resolved by SDS-PAGE, transferred onto PVDF membrane and probed with anti-CD3 ϵ and anti-CD3 ζ . **(c)** Splenocytes were counted and stained with antibodies against TCR- β , B220, CD4 and CD8 for flow cytometric analysis. Cells were gated on total live or live/GFP⁺ cells. Numbers of T- and B-cell populations were calculated per 10⁷ GFP⁺ cells. The upper right box indicates the vectors used, recipient bone marrow (in parentheses) and the total percentage of GFP⁺ cells. Data represent the mean \pm s.e.m. of three to four mice per group. **(d)** Splenocytes were analyzed as in **c** and TCR expression on GFP⁺CD4⁺ and GFP⁺CD8⁺ T cells is shown. Numbers represent the mean fluorescence. The vectors and recipient bone marrow (in parentheses) used is shown on the left. A representative histogram is shown from three to four mice per group. **(e)** Splenocytes were stimulated with plate-bound anti-TCR-C β and proliferation measured by ³H-thymidine incorporation. The vectors and recipient bone marrow (in parentheses) used is shown. Data represent the mean \pm s.e.m. of three to four mice per group.

equine encephalitis virus-based vectors. In our hands, 2A peptides mediated efficient cleavage in all the constructs tested. Given that this is a structure-based event⁵, cleavage efficiency may be influenced by the protein that is attached to the N terminus of the 2A peptide. Therefore, the efficiency of this system would need to be determined empirically.

Several difficulties have been reported in the use of IRES elements and additional promoters in multicistronic vectors. The larger size of IRES elements and additional promoters, compared with 2A sequences, can be a substantial limitation for vectors with limited cloning capacity, such as rAAV and retroviral vectors¹⁴ and may also lead to reduced viral titers¹⁵. Additionally, internal promoters can be downregulated in retroviral vectors through promoter interference¹⁶. Furthermore, the use of multiple IRES elements can lead to competition for translation factors and/or homologous recombination¹⁷ and can vary profoundly in different cell types¹⁸. Lastly, IRES-dependent expression can be significantly lower than cap-dependent expression¹⁹. All of these problems are reduced or eliminated with the use of 2A peptide-based vectors. Particularly appealing aspects of this technology are the very small size of the 2A peptides and the fact that this

cleavage event does not appear to be influenced by external factors, as is seen with internal promoters and IRES. In addition, we have effectively used the 2A peptide as a tag for protein identification using an anti-2A peptide antisera (data not shown). A potential drawback of this system is the possibility that the small, 2A tag left at the end of the N-terminal protein may affect protein function or contribute to the antigenicity of the proteins. However, we have not yet observed these problems in our studies.

Expression of multiple proteins from a single vector could have multiple benefits. For example, cancer therapy vectors designed to express multiple drug-resistance genes in hematopoietic cells would help reduce the cytotoxic effects of chemotherapy²⁰. The expression of multiple suicide, antiangiogenic and/or immunoreactive proteins could substantially enhance gene therapy approaches to tumor treatment^{21,22}. The use of 2A peptide-based vectors could also improve the production efficiency of heteromultimeric proteins, such as immunoglobulins, cell surface receptors and cytokines (e.g., IL-12)^{23,24}. Thus, 2A peptide-based vectors could be very useful in both gene therapy and biomedical research where reliable, multi-protein expression is required.



METHODS

Generation of multicistronic vectors. Constructs were produced by recombinant PCR using the primers and scheme outlined in **Supplementary Figure 1** online²⁵. The constructs were cloned into either pCIneo (Promega) or an MSCV-based retroviral vector that contains an IRES and GFP, YFP or CFP⁷. Vectors used in FRET studies were constructed in two steps. First, a set of overlapping oligonucleotides (42–129 amino acids in length, see **Supplementary Fig. 4** online) was used to generate a codon-diversified YFP (YFP^{CD}) by recombinant PCR. This product was used to replace the native YFP in MSCV-IRES-YFP by digestion with *Nco*I and *Not*I. Second, CFP was then generated by PCR using a 5' primer with an *Eco*RI site and a 3' primer encoding either the P2A sequence (see **Fig. 1a**) or a flexible linker (GGSGGGGGSS) with an *Nco*I site identical in reading frame to that found at the YFP start codon. These products were then used to replace the IRES segment to generate the constructs depicted in **Figure 4a**. No differences in fluorescent properties of YFP and YFP^{CD} were seen (data not shown). Oligonucleotide sequences are depicted in **Supplementary Figures 1** and **4**.

Mice. CD3 $\zeta^{-/-}$, RAG-1 $^{-/-}$ and C57BL/6 mice were obtained from Jackson Laboratories. CD3 $\epsilon^{\Delta P/\Delta P}$ (ref. 11) mice were provided by Cox Terhorst (Harvard Medical School). All animal experiments were performed in an AAALAC-accredited, SPF facility following national, state and institutional guidelines. Animal protocols were approved by St. Jude Institutional Animal Care and Use Committee.

Transient transfection of 293T cells. Transfections were performed as described with some modifications¹⁰. 293T cells (human embryonic kidney cells; provided by David Baltimore) were incubated in 10-cm plates at 2×10^6 /plate overnight at 37 °C. Cells were transiently transfected with 2 μ g DNA for each construct using Fugene (Roche). After a 2-d incubation, cells were stained with anti-TCR- β .PE (H57-597) and anti-CD3 ϵ .APC (2C11) (BD Pharmingen) and analyzed by flow cytometry.

Generation of retroviral producer cells and stable transduction of 3T3 cells. Retrovirus producer cell lines were generated as described with some modifications^{26–28}. 293T cells were transiently transfected using Fugene. Retroviral producer cell lines were then generated by repeatedly transducing GP+E86 cells²⁶ (6–8 times) until a viral titer of greater than 10^5 /ml after 24 h was obtained. 3T3 cells were transduced with 200 μ l supernatant from the appropriate retroviral producer cell line for each construct twice a day for 3 d in the presence of polybrene (hexadimethrine bromide; 6 μ g/ml) (Sigma). Cells were stained with antibodies against TCR:CD3 and analyzed by flow cytometry.

Retroviral-mediated stem cell gene transfer. Retroviral transduction of murine bone marrow cells was done as described²⁷. Briefly, bone marrow was harvested from 10- to 15-week-old donor mice, 48 h after treatment with 150 mg/kg 5-fluorouracil (5-FU; Pharmacia). Bone marrow cells were cultured in medium and the stem cells induced to proliferate with 20 ng/ml murine interleukin-3 (IL-3), 50 ng/ml human interleukin-6 (IL-6) and 50 ng/ml murine stem cell factor (SCF) (R&D Systems). Bone marrow cells were cocultured for 48 h with the retroviral producer cell lines described above. The nonadherent, transduced bone marrow cells were collected and washed. Sublethally irradiated (900 rads) recipient mice were injected via the tail vein with 4×10^6 bone marrow cells in PBS with 2% FBS and 20 u/ml heparin. Mice were analyzed 8–10 weeks post-transplant. Splenocytes from CD3-reconstituted mice were stained with the following antibodies: anti-TCR- β .PE (H57-597), anti-CD45R/B220-APC (RA3-6B2), anti-CD4.APC (RM4-4) or anti-CD4-cychrome and anti-CD8.PE (53-6.7) (BD Pharmingen).

In vitro transcription and translation. Coupled *in vitro* transcription and translation was performed using TNT Coupled Wheat Germ Extract System and Transcend Non-Radioactive Translation Detection System according to manufacturer's instructions (Promega). Constructs encoding single CD3 chains or the 2A peptide-linked molecules were cloned into pCIneo vector (Promega). A noncleaving version of T2A peptide was created by mutation of the last proline and glycine of the 2A peptide to alanine (**Fig. 1a**, underlined). Translated proteins were detected using biotinylated lysine incorporation as per instructions and run on a 12% SDS-PAGE gel. Proteins were detected using streptavidin-biotinylated horseradish peroxidase and ECL Plus (Amersham). Location of CD3 δ and CD3 γ was confirmed by probing with antisera raised against C-terminal peptides derived from CD3 δ (KNEQLYQ-PLRDREDTQYSRLGGNWP RNKKS) or CD3 γ (EYDQYSHLQGNQLRKK) (Covance Research Products). Because the CD3 δ peptide immunogen is longer, some cross-reactivity was seen with the anti-CD3 δ antisera against the CD3 γ protein.

Surface biotinylation, immunoprecipitation and immunoblotting. Cells were surface biotinylated, as previously described¹⁰. Briefly, 1×10^7 cells were washed in Hank's balanced salt solution (HBSS) and labeled with 1 mg/ml NHS-SS-biotin (Pierce Chemical) in HBSS for 30 min on ice. Excess biotin was quenched and cells were washed two times in 20 mM L-lysine. Cells were lysed in 1% digitonin and the lysate precleared with heat-killed, formalin-fixed *Staphylococcus aureus* (Pansorbin) cells (Calbiochem). The lysate was immunoprecipitated with protein G sepharose (Pharmacia) precoated with anti-TCR- β (H57-597). Eluted proteins were resolved by 10% SDS-PAGE and transferred onto polyvinylidene fluoride (PVDF) membrane. Membranes were probed with

streptavidin-AP and developed using Vistra substrate (Amersham). Membranes were stripped and reprobed with anti-CD3 ζ (H146-968), anti-CD3 ϵ (HMT3.1), anti-CD3 γ (H25-1157.17) and anti-TCR α (H28-710). Antibody binding was detected using Protein A/G-AP and densitometric analysis was performed with ImageQuant (Amersham).

Proliferation assay. Splenocytes (5×10^5 /well) were cultured in 96-well flat-bottom plates precoated overnight with anti-TCR- β (H57-597; threefold dilutions from 5 μ g/ml)²⁹. On day 2, proliferation was measured by pulsing with ³H-thymidine (1 μ Ci/well; DuPont) for 24 h.

FRET analysis. Mice used in FRET analysis were generated by retroviral-mediated stem cell gene transfer as described above. C57BL/6 mice were used as donors and sublethally irradiated RAG-1^{-/-} mice were recipients. As controls for flow cytometric analysis, additional mice were generated that expressed CFP or YFP^{CD} alone. Six to eight weeks post-transfer, thymus, spleen, blood and bone marrow from these mice were collected and analyzed by flow cytometry after staining with biotinylated-, APC- and/or PerCP-Cy5.5-conjugated antibodies against the following: TCR- β , B220, TCR $\gamma\delta$ (GL3), CD3 ϵ , CD49b (NK cells), Mac1 (CD11b; macrophages), Gr-1 (Ly-6G and Ly-6C; granulocytes), TER119 (erythroid cells), lineage markers (Lin cocktail: CD5, B220, Mac-1, Gr-1, TER119, and 7-4; Stem Cell Technologies), CD34 and c-Kit (all antibodies from BD Pharmingen except where stated). Cells were analyzed on an LSR II flow cytometer (Becton Dickinson) using the following laser wavelengths and filter sets: 488-nm wavelength laser with 488/10 (forward scatter and side scatter), 550/20 (YFP) and 695/40 (PerCP-CY5.5) band-pass filters; 405-nm wavelength laser with 475/16 (CFP) and 550/20 (YFP FRET) filters; and 633-nm wavelength laser with 660/20 filter (APC). For western blot analysis, splenic B cells from CFP-2A-YFP^{CD} recipients were sorted on CFP⁺YFP^{CD}⁺ high and low fluorescent populations. Cells were lysed in 1% NP40 and proteins were resolved by 12% SDS-PAGE along with a recombinant GFP standard (5 μ g) (BD Clontech) and transferred onto PVDF membrane. Membranes were probed with an anti-GFP antibody that recognizes GFP and its YFP and CFP variants (A.v. monoclonal antibody, JL-8; BD Clontech). Antibody binding was detected using protein A/G-AP and ECF (Amersham), and densitometric analysis was done with ImageQuant (Amersham).

Note: Supplementary information is available on the Nature Biotechnology website.

ACKNOWLEDGMENTS

We are very grateful to Cox Terhorst and David Baltimore for reagents and Terry Geiger for his critical review of the manuscript. We also wish to thank Richard Cross, Jennifer Hoffrage, Richard Ashmun and Ann-Marie Hamilton-Easton for assistance with flow cytometry, staff in the Hartwell Center for oligo synthesis and DNA sequencing, and members of the Vignali lab for constructive criticism, comments and bone marrow isolation. This work was supported by grants from the National Institutes of Health (AI39480, AI52199), a Cancer Center Support CORE grant (CA-21765) and the American Lebanese Syrian Associated Charities to D.A.A.V.

COMPETING INTERESTS STATEMENT

The authors declare that they have no competing financial interests.

Received 4 December 2003; accepted 20 January 2004

Published online at <http://www.nature.com/naturebiotechnology/>

- Ryan, M.D. & Flint, M. Virus-encoded proteinases of the picornavirus super-group. *J. Gen. Virol.* **78**, 699–723 (1997).
- Palmenberg, A.C. *et al.* Proteolytic processing of the cardioviral P2 region: primary 2A/2B cleavage in clone-derived precursors. *Virology* **190**, 754–762 (1992).

- Donnelly, M.L. *et al.* The 'cleavage' activities of foot-and-mouth disease virus 2A site-directed mutants and naturally occurring '2A-like' sequences. *J. Gen. Virol.* **82**, 1027–1041 (2001).
- Ryan, M.D., King, A.M. & Thomas, G.P. Cleavage of foot-and-mouth disease virus polyprotein is mediated by residues located within a 19 amino acid sequence. *J. Gen. Virol.* **72**, 2727–2732 (1991).
- Donnelly, M.L. *et al.* Analysis of the aphthovirus 2A/2B polyprotein 'cleavage' mechanism indicates not a proteolytic reaction, but a novel translational effect: a putative ribosomal 'skip'. *J. Gen. Virol.* **82**, 1013–1025 (2001).
- Klausner, R.D., Lippincott-Schwartz, J. & Bonifacio, J.S. The T cell antigen receptor: insights into organelle biology. *Annu. Rev. Cell Biol.* **6**, 403–431 (1990).
- Persons, D.A. *et al.* Use of the green fluorescent protein as a marker to identify and track genetically modified hematopoietic cells. *Nat. Med.* **4**, 1201–1205 (1998).
- Vanin, E.F. *et al.* Development of high-titer retroviral producer cell lines by using Cre-mediated recombination. *J. Virol.* **71**, 7820–7826 (1997).
- Julias, J.G., Hash, D. & Pathak, V.K. E-vectors: development of novel self-inactivating and self-activating retroviral vectors for safer gene therapy. *J. Virol.* **69**, 6839–6846 (1995).
- Liu, H.Y., Rhodes, M., Wiest, D.L. & Vignali, D.A.A. On the dynamics of TCR:CD3 complex cell surface expression and downmodulation. *Immunity* **13**, 665–675 (2000).
- Wang, B. *et al.* T lymphocyte development in the absence of CD3 ϵ or CD3 $\gamma\delta\zeta$. *J. Immunol.* **162**, 88–94 (1999).
- Love, P.E. *et al.* T cell development in mice that lack the zeta chain of the T cell antigen receptor complex. *Science* **261**, 918–921 (1993).
- Chan, F.K. *et al.* Fluorescence resonance energy transfer analysis of cell surface receptor interactions and signaling using spectral variants of the green fluorescent protein. *Cytometry* **44**, 361–368 (2001).
- de Felipe, P., Martin, V., Cortes, M.L., Ryan, M. & Izquierdo, M. Use of the 2A sequence from foot-and-mouth disease virus in the generation of retroviral vectors for gene therapy. *Gene Ther.* **6**, 198–208 (1999).
- Klump, H. *et al.* Retroviral vector-mediated expression of HoxB4 in hematopoietic cells using a novel coexpression strategy. *Gene Ther.* **8**, 811–817 (2001).
- Emerman, M. & Temin, H.M. Genes with promoters in retrovirus vectors can be independently suppressed by an epigenetic mechanism. *Cell* **39**, 449–467 (1984).
- Wang, S., Beattie, G.M., Hayek, A. & Levine, F. Development of a VSV-G protein pseudotyped retroviral vector system expressing dominant oncogenes from a lacO-modified inducible LTR promoter. *Gene* **182**, 145–150 (1996).
- Borman, A.M., Le Mercier, P., Girard, M. & Kean, K.M. Comparison of picornaviral IRES-driven internal initiation of translation in cultured cells of different origins. *Nucleic Acids Res.* **25**, 925–932 (1997).
- Mizuguchi, H., Xu, Z., Ishii-Watabe, A., Uchida, E. & Hayakawa, T. IRES-dependent second gene expression is significantly lower than cap-dependent first gene expression in a bicistronic vector. *Mol. Ther.* **1**, 376–382 (2000).
- Sorrentino, B.P. Gene therapy to protect hematopoietic cells from cytotoxic cancer drugs. *Nat. Rev. Cancer* **2**, 431–441 (2002).
- Pizzato, M. *et al.* Production and characterization of a bicistronic Moloney-based retroviral vector expressing human interleukin 2 and herpes simplex virus thymidine kinase for gene therapy of cancer. *Gene Ther.* **5**, 1003–1007 (1998).
- Moriuchi, S. *et al.* Enhanced tumor cell killing in the presence of ganciclovir by herpes simplex virus type 1 vector-directed coexpression of human tumor necrosis factor- α and herpes simplex virus thymidine kinase. *Cancer Res.* **58**, 5731–5737 (1998).
- Kessels, H.W., Wolkers, M.C., van, D.B., van der Valk, M.A. & Schumacher, T.N. Immunotherapy through TCR gene transfer. *Nat. Immunol.* **2**, 957–961 (2001).
- Zitvogel, L. *et al.* Construction and characterization of retroviral vectors expressing biologically active human interleukin-12. *Hum. Gene Ther.* **5**, 1493–1506 (1994).
- Vignali, D.A.A. & Vignali, K.M. Profound enhancement of T cell activation mediated by the interaction between the T cell receptor and the D3 domain of CD4. *J. Immunol.* **162**, 1431–1439 (1999).
- Markowitz, D., Goff, S. & Bank, A. A safe packaging line for gene transfer: separating viral genes on two different plasmids. *J. Virol.* **62**, 1120–1124 (1988).
- Persons, D.A. *et al.* Retroviral-mediated transfer of the green fluorescent protein gene into murine hematopoietic cells facilitates scoring and selection of transduced progenitors in vitro and identification of genetically modified cells *in vivo*. *Blood* **90**, 1777–1786 (1997).
- Persons, D.A., Mehaffey, M.G., Kaleko, M., Nienhuis, A.W. & Vanin, E.F. An improved method for generating retroviral producer clones for vectors lacking a selectable marker gene. *Blood Cells Mol. Dis.* **24**, 167–182 (1998).
- Carson, R.T., Vignali, K.M., Woodland, D.L. & Vignali, D.A. T cell receptor recognition of MHC class II-bound peptide flanking residues enhances immunogenicity and results in altered TCR V region usage. *Immunity* **7**, 387–399 (1997).

Erratum: Erbitux diagnostic latest adjunct to cancer therapy

Peter Mitchell

Nat. Biotechnol. 22, 363–364 (2004)

On page 363, column 2, line 14, sepsis is incorrectly listed as one of the side effects of Erbitux. The sentence should have read “potential side effects such as rare cases of interstitial lung disease.”

Corrigendum: Correction of multi-gene deficiency *in vivo* using a single ‘self-cleaving’ 2A peptide–based retroviral vector

Andrea L Szymczak, Creg J Workman, Yao Wang, Kate M Vignali, Smaroula Dilioglou, Elio F Vanin & Dario AA Vignali

Nat. Biotechnol. 22, 589–594 (2004)

In Figure 3b, the labels for CD3e and CD3e-2A were inverted. Thus, the second band should have been labeled CD3e-2A and the third band labeled CD3e.

Corrigendum: The potential environmental impact of engineered nanomaterials

Vicki L Colvin

Nat. Biotechnol. 21, 1166–1170 (2003)

In the Acknowledgments, line 3, the name Cafer Yavuz was misspelled as Cafer Tevuyz.

Addendum: Correction of multi-gene deficiency *in vivo* using a single ‘self-cleaving’ 2A peptide–based retroviral vector

Andrea L Szymczak, Creg J Workman, Yao Wang, Kate M Vignali, Smaroula Dilioglou, Elio F Vanin & Dario AA Vignali

Nat. Biotechnol. 22, 589–594 (2004)

Technical note: Recent experiments with other 2A-linked constructs have suggested that cleavage efficiency can be influenced by the protein NH₂-terminal to the 2A peptide. In some instances, we have found that cleavage efficiency can be improved by placing a Gly-Ser-Gly linker between NH₂-terminal protein and the 2A peptide.